Hindawi
Advances in Materials Science and Engineering
Volume 2019, Article ID 1321780, 11 pages
https://doi.org/10.1155/2019/1321780

Research Article

Simulation of Material Removal Process in EDM with Composite Tools

Shengfang Zhang,[1] **Wenchao Zhang**,[1] **Puyong Wang**,[2] **Yu Liu**,[1] **Fujian Ma**,[1] **Dapeng Yang**,[1] **and Zhihua Sha**[1]

[1]*School of Mechanical Engineering, Dalian Jiaotong University, Dalian 116028, China*
[2]*CRRC Changchun Railway Vehicles Co., Ltd., Changchun 130062, China*

Correspondence should be addressed to Yu Liu; liuyu_ly12@126.com

Received 23 November 2018; Accepted 15 January 2019; Published 24 February 2019

Academic Editor: Joon-Hyung Lee

With the development of (electrical discharge machining) EDM technology, composite tools with special features gradually replace the traditional single-material tools and have become widely used in specific processing conditions. In order to predict the wear of composite tool effectively, in this paper, a material removal model of single-pulse EDM with composite tools was established by using the finite element method. The surface temperature distribution of the composite tool was obtained by taking the copper-die steel tool as the analysis object. And the shape of discharge crater as well as the removal volume was obtained by the element birth and death method. The influences of discharge parameters and tool materials on the removal volume were analyzed respectively. The EDM experiments were carried out by using copper-die steel as the composite tool to verify the simulation results. It shows that the errors between actual machining results and the simulation results are less than 10%, which proves the accuracy of the simulation model.

1. Introduction

In aerospace, biomedical, optoelectronic communication, mold manufacturing, and many other fields, due to the special working environment, many key parts often use difficult-to-cut materials, which are difficult to process with traditional machining method for high precision. Electrical discharge machining (EDM), using the electrothermal effect of pulsed spark discharge between tool and workpiece to remove materials in a dielectric fluid, has the advantages of noncontact machining, low cost, and wide adaptability. It is widely used in small hole and cavity machining of difficult-to-cut materials. However, because of the high tool wear and large-shape change in EDM using traditional single-material tools, some kinds of composite tools are introduced to meet the increasing requirements of high accuracy and low tool wear during machining process. There are many scholars studying the machining performances of EDM with a variety of composite tools which consist of different materials.

Extensive researches have been carried out on EDM with composite electrodes. Norasetthekul et al. coated the brass tool surface with a layer of thick materials which has a high melting point and good thermal conductivity to make a composite tool. The working life of the composite tool can be 3–5 times than that of the brass tool and the copper-tungsten tool, and the price is lower than the graphite tool; besides, the machining surface quality was improved [1]. Tsai et al. prepared the Cr-Cu composite tool by sintering the resin mixture of Cu and Cr powder at lower temperature (200°C) and lower pressure (20 MPa), and this method could change the performance of the composite tool by adjusting the sintering temperature and the static pressure [2]. Khanra et al. developed a ZrB_2-Cu composite electrode and found the composite tool shows more metal removal rate with less tool removal rate than Cu tool [3]. El-Taweel investigated the relationship between process parameters in electrodischarge of CK45 steel and tool electrode material as Al-Cu-Si-TiC composite is produced using the powder metallurgy (P/M) technique. The central composite second-order rotatable design had been utilized to plan the experiments, and response surface methodology (RSM) was applied to develop experimental models. Al-Cu-Si-TiC P/M electrodes are

found to be more sensitive to peak current and pulse on time than traditional electrodes [4]. Hassan et al. made research on the fabrication of metal matrix composite electrode by mixing copper power with Al_2O_3 power [5]. Senthilkumar and Reddy developed a new copper-based metal matrix composite (Cu-B_4C) for an EDM electrode to get an optimum combination of wear resistance and electrical and thermal conductivity. The results showed that copper composite with 40% boron carbide reinforcement showed a better material removal rate (MRR) and tool wear rate (TWR) compared to the conventional copper electrode [6]. Goyal performed using composite material electrode on Die steel EN-31 and found that copper-manganese (weight ratio: 70–30) composite electrode shows better results than copper-manganese (weight ratio: 80–20) electrode for MRR [7]. Chiou et al. presented a comparative study of the performance of WC, WC-coated Ag, and WC-coated Cu electrodes for the micro-EDM milling, and the experimental results showed that the WC-coated Ag electrodes yielded the lowest surface roughness and the WC-coated Cu electrodes achieved the highest material removal rate, which showed the effectiveness of the electrode coating method [8]. Hussain fabricated copper and novel material aluminum oxide/copper (Al_2O_3/Cu) composite using powder metallurgy technique. It was found that wear rate is highly depending on hardness, mass density, and green protective carbonate layer formation at the surface of the composite [9]. Zhang et al. presented the multimaterial tool EDM processing method and the use of different wear characteristics of different tool materials, EDM small complex surfaces can be obtained by EDM sinking, the method can avoid the shortcomings of traditional layered milling method, such as low processing efficiency, tool replacement, and the complex tool path planning strategy [10].

In summary, previous researchers have done lots of analysis and studies on the tool wear in EDM and have obtained many excellent research results; however, studies on the material removal of composite tool wear process and other issues are less, and composite tool wear will affect the machining accuracy and processing efficiency of EDM. This paper mainly focuses on finite element analysis of tool material erosion process of composite tools in EDM.

2. Model Establishment and Analysis

2.1. Mathematical Model of Electrothermal Conversion. EDM is composed of countless single-pulse discharge process. Each discharge process includes dielectric breakdown, discharge channel formation, material removal, and intertool deionization. The instantaneous high temperature produced by the discharge channel makes the tool material molten or even vaporized; meanwhile, the produced instantaneous pressure change will eject the debris into dielectric working fluid. At the end of the pulse discharge, the dielectric between the two electrodes deionizes and restores insulation.

The main reason for the formation of the two-electrode temperature field during the EDM process is the interelectrode heat source. Most of the energy during discharge is distributed in the form of heat energy on the positive and negative tools. It forms the transient high-temperature heat sources. The instantaneous heat sources include volume heat sources and surface heat sources, the volume heat source is mainly determined by the skin effect, and material removal by the volume heat source is only 1% to 2% of the total amount. So, the surface heat source is the main factor of material removal. In this paper, the heat generated during discharge is considered as a surface heat source, and the heat flux q can be expressed by [11–13]

$$q(r) = q_0 \exp\left[-4.5\left(\frac{r}{R}\right)^2\right], \tag{1}$$

where q_0 is the heat flux, r is the distance between the discharge point and the center in the channel, and R is the discharge radius. It is assumed that the energy of a single-pulse discharge can only form an effective spark discharge. Considering the Gaussian heat flux at time t, the heat flux density expression at r is given as follows:

$$q(r,t) = \frac{4.45\eta U_b(t) I(t)}{\pi R^2} \exp\left[-4.5\left(\frac{r}{R}\right)^2\right], \tag{2}$$

where η is the heat flux distribution coefficient, $U_b(t)$ is the discharge voltage between the electrodes, and $I(t)$ is the peak current. Figure 1 shows the heat flux loading model under single-pulse conditions.

The convective heat equation is as follows:

$$Q_c = hA(T - T_0), \tag{3}$$

where Q_c is the heat transferred per unit time, h is the heat transfer coefficient, A is the area of the object, T is the object's surface temperature, and T_0 is the fluid temperature.

In Figure 1, the area of $r \le R$ is the heat flux input region, and the area of $r > R$ is the convective heat transfer region; other boundary conditions are ambient temperature. In EDM, due to the continuous input of heat, the entire thermal conduction process is dynamic, and the temperature field is the transient temperature field. The boundary conditions are satisfying the convective heat conduction in the liquid-phase region and the Fourier heat transfer formula in the solid phase region.

Figure 2 shows the heat flux applied to the surface of the composite electrode. Assume that the center of the heat source is at the origin of the coordinate, the heat source emits heat Q_t, ignore the conduction of heat to the air above the object, and the heat only conducts on the surface of the plane XOY and in the negative direction of the axis Z. Take the extremely small width dx, the length dy, and the height dz near the heat source to form an effective heat generating region, the temperature in the extremely small volume region can be solved.

Since heat is a function of time t, Fourier unsteady heat conduction differential equations are applied in three-dimensional Cartesian coordinates, and energy conservation equations and boundary conditions are considered as follows [14, 15]:

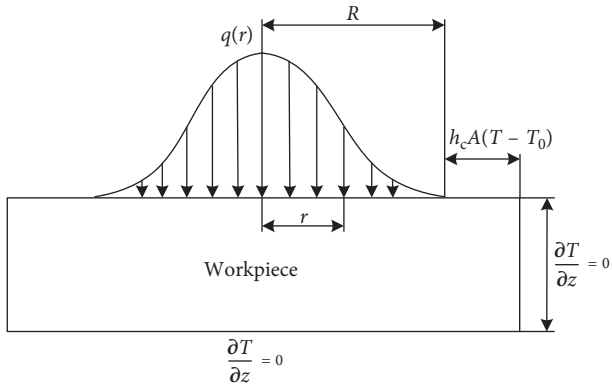

Figure 1: Single-pulse heat flux application model.

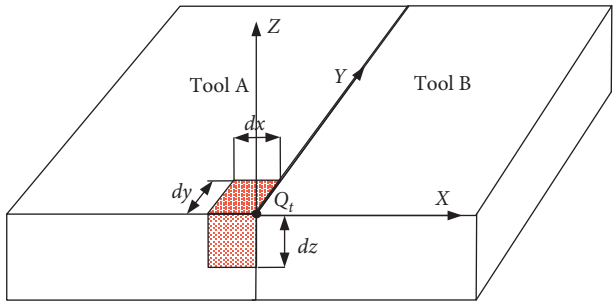

Figure 2: Heat source on the tool surface.

$$\frac{\partial\theta}{\partial t} = \frac{\lambda}{c\rho}\left(\frac{\partial^2\theta}{\partial x^2} + \frac{\partial^2\theta}{\partial y^2} + \frac{\partial^2\theta}{\partial z^2}\right), \tag{4}$$

$$Q_t = \int_0^c \int_0^b \int_0^a \theta(x, y, z, t) c\rho \; dx \; dy \; dz, \tag{5}$$

$$\theta(x, y, z, t)\big|_{t=0} = 0, \tag{6}$$

where t is the time, $\theta(x, y, z, t)$ is the time-dependent and position-dependent temperature, c is the specific heat capacity, ρ is the density of electrodes, λ is the conductivity coefficient, and a, b, and c is the extremely small region.

The Fourier transform method is applied and equations (7)–(9) are as follows:

$$\mathcal{F}\left\{\frac{\partial^2\theta}{\partial x^2}\right\} = (i\alpha)^2\mathcal{F} = -\alpha^2\mathcal{F}, \tag{7}$$

$$\mathcal{F}\left\{\frac{\partial^2\theta}{\partial y^2}\right\} = (i\beta)^2\mathcal{F} = -\beta^2\mathcal{F}, \tag{8}$$

$$\mathcal{F}\left\{\frac{\partial^2\theta}{\partial z^2}\right\} = (i\gamma)^2\mathcal{F} = -\gamma^2\mathcal{F}, \tag{9}$$

where $F(\alpha, \beta, \gamma, t)$ is the Fourier transform of $\theta(x, y, z, t)$. Equation (10) is obtained according to equations (4) and (7)–(9) with the Fourier transform method:

$$\frac{\partial F}{\partial t} = -a\left(\alpha^2 + \beta^2 + \gamma^2\right)\mathcal{F}, \tag{10}$$

where $a = \lambda/c\rho$. After transforming, the left and right sides of equation (10) are integrated to obtain

$$F(\alpha, \beta, \gamma, t) = Ae^{-at\left(\alpha^2+\beta^2+\gamma^2\right)}. \tag{11}$$

Inverse Fourier transform method is applied on equation (11) to obtain

$$\theta(x, y, z, t) = A\left[\frac{1}{2\pi}\int_{-\infty}^{+\infty} e^{-at\alpha^2}e^{-i\alpha x}d\alpha\right] \cdot \left[\frac{1}{2\pi}\int_{-\infty}^{+\infty} e^{-at\beta^2}e^{-i\beta y}d\beta\right] \cdot \left[\frac{1}{2\pi}\int_{-\infty}^{+\infty} e^{-at\gamma^2}e^{-i\gamma y}d\gamma\right]. \tag{12}$$

Equation (12) is integrated to obtain

$$\theta(x, y, z, t) = \frac{A}{(2\pi)^2}\frac{\sqrt{\pi}}{\sqrt{at}}e^{-\left(x^2/(4at)\right)}\frac{\sqrt{\pi}}{\sqrt{at}}e^{-\left(y^2/(4at)\right)} \cdot \frac{\sqrt{\pi}}{\sqrt{at}}e^{-\left(z^2/(4at)\right)} = \frac{A}{4\pi at}e^{-\left(\left(x^2+y^2+z^2\right)/(4at)\right)}. \tag{13}$$

Substitute $\theta(x, y, z, t)$ for equation (5) to obtain

$$Q_t = \frac{A}{4\pi at}\int_0^c \int_0^b \int_0^a e^{-\left(\left(x^2+y^2+z^2\right)/(4at)\right)} c\rho \; dx \; dy \; dz. \tag{14}$$

Coefficient A can be obtained:

$$A = \frac{4\pi atQ_t}{\int_0^c \int_0^b \int_0^a e^{-\left(\left(x^2+y^2+z^2\right)/(4at)\right)} c\rho \; dx \; dy \; dz}. \tag{15}$$

Substitute A in equation (13) to obtain a temperature rise equation of the tool:

$$\theta(x, y, z, t) = \frac{\eta Q_t}{c\rho \int_0^a e^{-(x^2/4at)}dx \int_0^b e^{-\left(y^2/4at\right)}dy \int_0^c e^{-(z^2/4at)}dz} \cdot e^{-\left(\left(x^2+y^2+z^2\right)/4at\right)}. \tag{16}$$

Since the heat is an accumulated process during the EDM process, the whole discharge process can be regarded as the accumulation of multiple single discharges, so the whole discharge time can be divided into many moments $d\tau_0$, $d\tau_1$, $d\tau_2$, $d\tau_3$,. . ., $d\tau_i$, and the whole time t is the sum of these discharge moments. Equation (17) is obtained as follows:

$$t = \int_{t0}^{t1} d\tau_i, \tag{17}$$

where $d\tau$ is the heating moment. The temperature rise caused by the continuous generation of heat during the machining process from t_0 to t_1 is obtained as follows:

$$\theta(x,y,z,t)=\int_{t0}^{t1}\frac{\eta Q_t}{c\rho\int_0^a e^{-(x^2/4at)}dx\int_0^b e^{-(y^2/4at)}dy\int_0^c e^{-(z^2/4at)}dz}\cdot e^{-((x^2+y^2+z^2)/4at)}d\tau_i. \tag{18}$$

Therefore, the final temperature changes of the workpiece can be solved by equation (18).

2.2. Selection of Materials and Simulation Modeling. The simulation is programmed by Ansys APDL language due to its convenience and powerful function. In order to clearly understand the removal volume and the surface appearance after the material removal, the element type of 3D node solid70 is applied. When the heat flux density and convection are applied simultaneously onto the same surface, one must be applied to the solid element and the other is applied to the surface effect element. In this paper, surface 152 is applied as the surface effect element. Since the composite tool is axisymmetric, only half of the model is used for the study. Each tool is set to a cube model with a side length as 30 μm. The mesh size is 0.5 μm, so the whole model is divided into 432000 elements. The two tool models are connected with "glue" command so that the heat can be conducted to each other in the simulation. When the single-pulse discharge removal of composite tools is simulated, the copper-die steel, graphite-die steel, and copper-graphite tools are selected as the composite tools. As the discharge of EDM is a complex process, modeling involves the use of some simplifying assumptions:

(1) Only one spark is considered in the analysis

(2) The materials are completely removed and no condensation phenomenon occurs

(3) Workpiece and tool material are homogeneous and isotropic in nature

The simulation parameters of composite tools are shown in Table 1.

Under normal temperature conditions, physical and thermal parameters such as thermal conductivity and specific heat capacity will not change too much, so their value changes are ignored. But in EDM process, each discharge machining time is very short and the heat flux applied to the surface of electrode is very high, which causes a large fluctuation in the temperature of the electrode. And the property parameters such as thermal conductivity, specific heat capacity, and other physical properties will change accordingly. At this point, taking the average value of the material property parameters will result in a large calculation error. In order to avoid this error, according to the existing data of the materials, the thermal conductivity and specific heat capacity shown in Tables 2–4 [16] at different temperatures are input into ANSYS. And then, an automatic interpolation operation will be performed in ANSYS to obtain the property parameter values at different temperatures.

Table 1: Simulation parameters of composite tools.

Parameters	Values
Materials of electrodes	Copper-die steel, graphite-die steel, copper-graphite
Machining polarity	Negative
Pulse on time	12, 16, and 20 μs
Breakdown voltage	20, 25, and 30 V
Peak current	1.2, 1.4, and 1.6 A

Table 2: Copper properties at different temperatures [16].

Temperature (K)	Coefficient of thermal conductivity (W/(m·K))	Specific heat (J/(kg·K))
298	385	384
373	377	393
473	367	414
573	358	422
673	349	431
773	341	443
873	334	456
973	330	468
1073	325	477
1273	317	498
1933	313	510

Table 3: Die steel properties at different temperatures [16].

Temperature (K)	Coefficient of thermal conductivity (W/(m·K))	Specific heat (J/(kg·K))
298	0.729	460
373	0.705	481
473	0.616	524
573	0.552	565
673	0.497	618
773	0.447	663
873	0.395	745
973	0.364	900
1073	0.355	1070
1273	0.342	1270
1933	0.331	2000

Table 4: Graphite properties at different temperatures [16].

Temperature (K)	Coefficient of thermal conductivity (W/(m·K))	Specific heat (J/(kg·K))
298	98	645
373	90	921
473	81	1189
573	73	1402
673	70	1540
773	59	1632
873	49	1695
973	45	1737
1073	39	1800
1273	36	1942
1933	32	1967

3. Simulation Results and Discussion

3.1. Temperature Distribution of Composite Tool. Because the tool temperature directly affects the erosion of the tool, the temperature distribution of the composite tool composed of copper-die steel is analyzed by simulation. Figure 3 shows the composite tool temperature contour and the composite tool surface temperature distribution curve along the radial direction when the voltage is 20 V, the current is 1.4 A, and the pulse width is 20 μs.

In Figure 3(a), the die steel tool is set on the left side of composite tool and the copper tool is on the right. It is found that the maximum temperature point deviates towards die steel tool instead of locating at the center of highest heat flux density. This is because that the thermal conductivity of copper is higher than that of die steel, although the specific heat capacity of copper is a bit lower than that of die steel. This leads that the temperature close to the center of heat flux density on die steel tool is increased faster after the heat flux density is applied to the junction of the die steel and copper. The temperature close to the center of heat flux density on the copper tool is increased slower, so there is a temperature difference. Due to the high temperature of die steel tool, the energy of the die steel tool will be conducted to the copper tool, and it leads to the temperature drop at the central point and does not achieve to the highest. The maximum temperature point deviates to die steel tool, which leads temperature of the place with highest heat flux density drop. Therefore, the temperature curve rises first and falls later as shown in Figure 3(b).

By the observation of Figure 3(c), it is shown that the highest temperature of composite tool approaches 4400 K and the temperature decreases as the radius increases. When $r < 0.6\,\mu$m, the temperature sharply drops, and when $r > 0.6\,\mu$m, the temperature drop becomes slow. The surface temperature of tool is of normal distribution conforming to the Gaussian distribution.

Comparing Figure 3(b) with Figure 3(c), it is shown that the edge temperature of the copper tool is higher than the die steel tool in composite tool. The reason is that the thermal conductivity of copper is better than die steel tool, and more energy is conducted to the edge of tool at the same time. So the temperature at the edge of the die steel tool is lower than the copper tool.

3.2. Impact of Discharge Parameters on Volume Removal. In order to calculate the size of crater on composite tool, composite tool composed of copper tool and die steel tool is considered, and the element birth and death method is adopted to deactivate the elements that is above the melting point in order to simulate the removal process in EDM. The number of deactivated elements is calculated, by which we multiplied the real size of the elements, so the removal volume could be obtained.

Set the melting temperature of copper tool as 1350 K and set the melting temperature of die steel tool as 1800 K. If the temperature is higher than the melting temperature, the element will be deactivated. Some simulation results under different discharge conditions are listed as shown in Figure 4 in which the left side of tool is die steel tool, and the right side is copper tool.

By observing Figure 4, it can be found that the remain surface after the material erosion is basically the same as the isothermal surface of each material. Each shape of the crater on the copper tool and the die steel tool is approximately similar to a one-eighth ball. But the shape of the crater on the die steel tool is larger than the one-eighth ball, while the shape of the crater on the copper tool is smaller than the one-eighth ball. The difference in shape is directly related to the phenomenon that the highest temperature point deviates to the steel side. It can also be found that although the same heat flux density is applied to the composite tools, the two tool materials have different tool wear.

Figures 5 and 6 are the composite tool wear volume change curves under different discharge parameter conditions, and it can be found that with the increasing of current, voltage, and pulse width, the wear volume of composite tool is increasing; this is because the heat flux is proportional to the current and voltage. The larger the discharge pulse width is and the longer the discharging time is, the more energy the tool can get, so material removal volume will increase. This conclusion is in accordance with the conclusion in [17]. But it can also be found that under the same conditions, in the composite tool, when the pulse width is small, the removed volume of die steel tool is higher than the copper tool. However, as the pulse width increases, the removed volume of die steel tool becomes lower than the copper tool. It is because although the die steel melting point is higher than copper, die steel thermal conductivity is poor and the energy conduction is slow, while the copper tool has excellent thermal conductivity, more energy is conducted away, resulting in a lower local temperature than die steel tool. When the input energy is not very high, the volume of die steel tool reaching the melting point is more than that of the copper tool because the heat conduction of copper carries away more energy, and then more elements of die steel tool are deactivated than copper. However, as the discharge energy continues to increase, although the volumes of die steel and copper tool are increasing correspondingly, the growth rate of copper tool is significantly larger than the die steel tool. It is because the thermal conductivity of copper tool is better than die steel, the energy is conducted to other copper elements quickly, and as the energy is large, more elements of copper tool will reach the melting point, which will be deactivated. Because of the poor thermal conductivity of die steel, even if the input energy is large enough, the number of elements which reach the melting point is not too many. Finally, when the input energy reaches a certain level, the amount of copper tool volume removal will be larger than that of the die steel tool.

3.3. Influence of Different Tool Material Combinations on Volume Removal. The tool wear is simulated when different tool materials are combined, and then the simulation results are analyzed. As shown in Figure 7, the craters under single

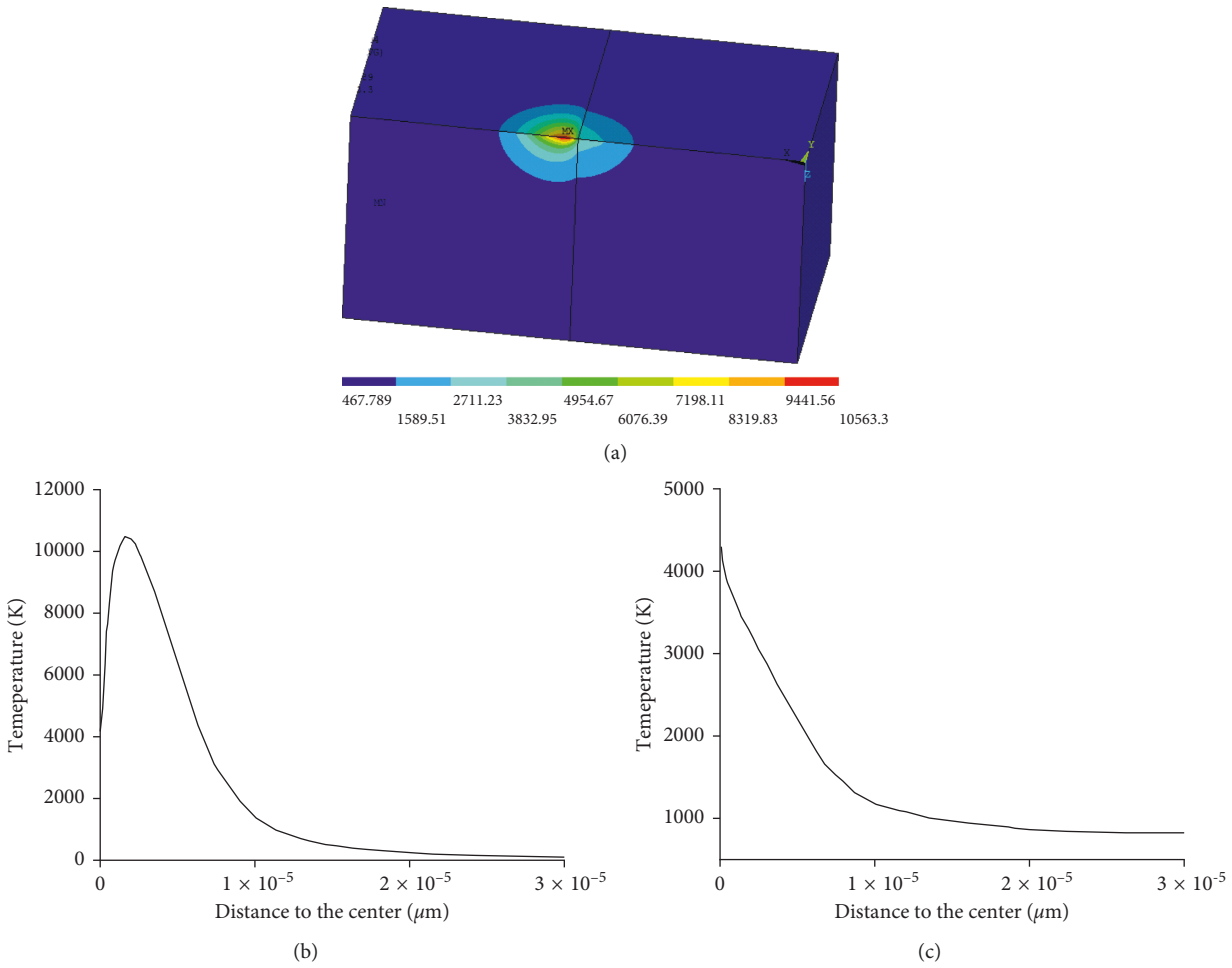

Figure 3: The temperature distribution of the composite tool. (a) Temperature contour of the composite tool. (b) The temperature curve of the die steel tool along the radius direction. (c) The temperature curve of the copper tool along the radius direction.

discharge conditions with different combinations of tool materials are obtained. Table 5 shows the tool wear with different combinations of tool materials at 20 V, 1.4 A, and 20 μs.

From Table 5, it can be found that if one tool material and another tool material are combined into one composite tool, under the same discharge condition, it will get different wear. For example, the graphite wear volume of graphite-die steel is more than that of graphite-copper. This is because graphite has a high melting point, and its thermal conductivity is lower than that of copper and die steel. Therefore, the temperature of the graphite at the heat source is higher than that of copper and die steel. And the energy is conducted from the graphite to the outside. The melting point of the die steel tool is higher than that of the copper, so the graphite-copper has a greater temperature difference, and the energy from the graphite to the copper is more than that conducted to the die steel tool. Moreover, the thermal conductivity of the copper is better than that of die steel tool, which further accelerates the energy conduction from the graphite to the copper tool in the graphite-copper tool; therefore, the energy of graphite in graphite-die steel is higher than the energy of graphite in the graphite-copper tool under the same condition, finally leading to higher wear of graphite in the graphite-die steel composite tool.

With the same discharge energy, a die steel single-material workpiece electrode is placed under the composite electrode to ensure that the discharge center of the workpiece electrode is just below the composite electrode, and the simulation is performed to make a comparative description about removal volume of the tool and the workpiece under a single discharge.

Figure 8 is the simulation result of die steel workpiece whose working condition is 20 V, 1.4 A, 20 μs. The melting point of die steel is close to 1800 K and the elements above the melting point are all deactivated. Since it is a single material, the lowest point of the discharge crater is directly below the center of the discharge point, and the shape of the discharge crater is relatively regular.

Figure 9 shows the temperature contour of the die steel workpiece. The highest temperature locates on the center point of the workpiece, reaching 12475 K. The temperature along the radius direction is decreased sharply at first then slowly to ambient temperature. This is because that the heat gathers near the center position and the instantaneous

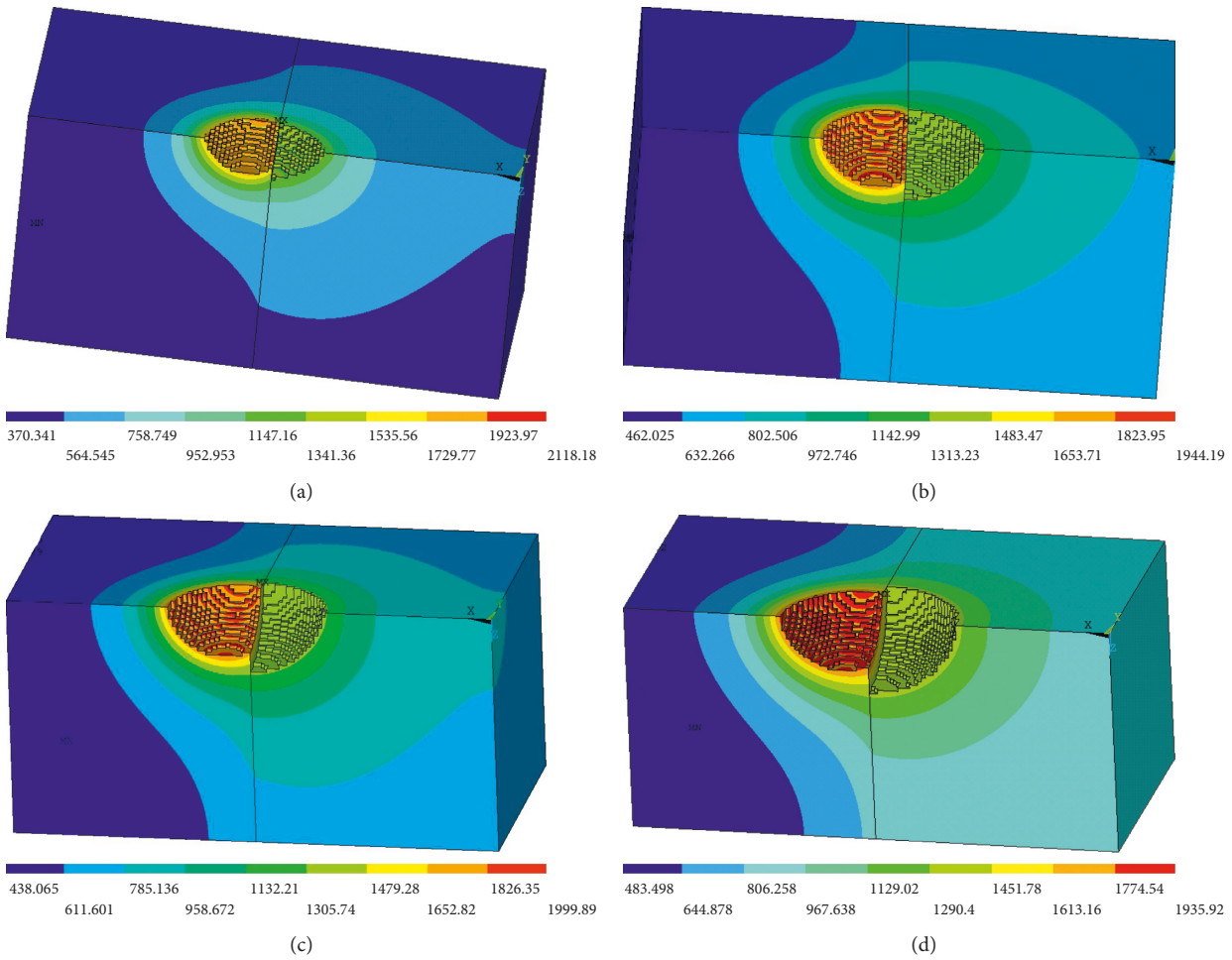

Figure 4: Craters of the composite tool under different discharge parameters. (a) Crater in the condition of 20 V, 1.2 A, and 20 μs. (b) Crater in the condition of 20 V, 1.4 A, and 20 μs. (c) Crater in the condition of 25 V, 1.4 A, and 16 μs. (d) Crater in the condition of 30 V, 1.6 A, and 20 μs.

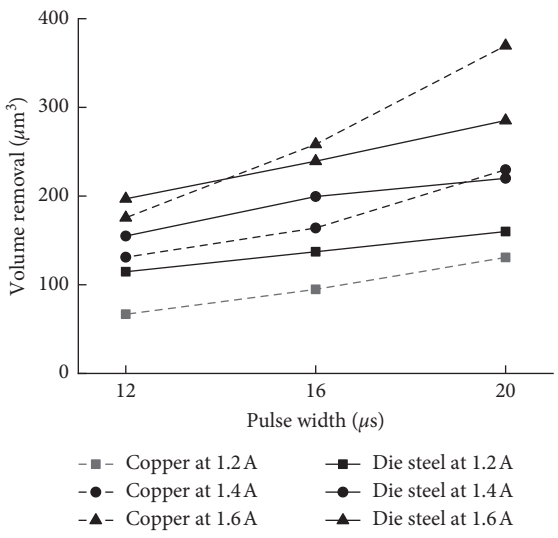

Figure 5: Volume removal with different pulse widths and voltages at 20 V.

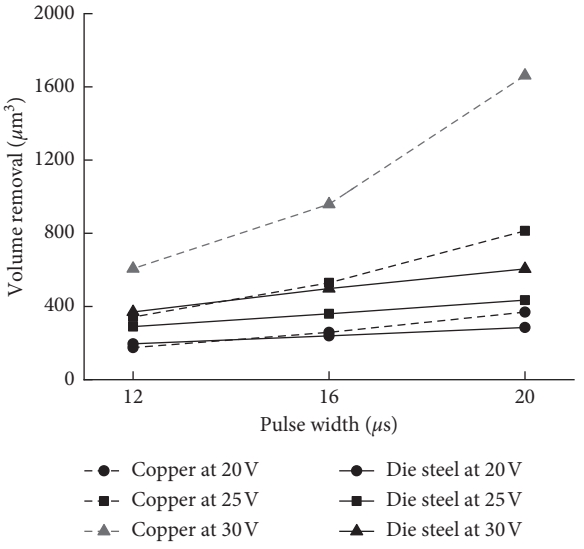

Figure 6: Volume removal with different pulse widths and voltages at 1.6 A.

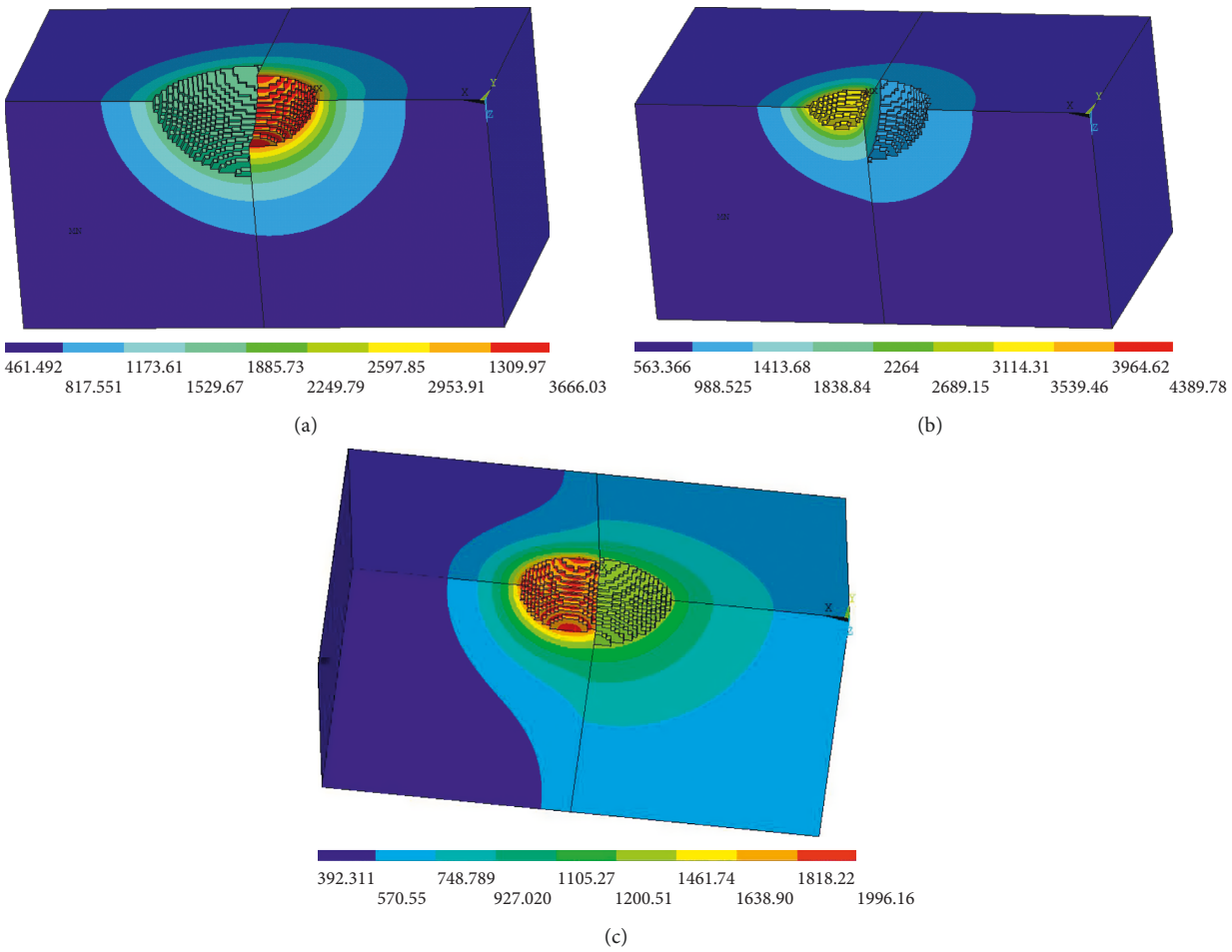

Figure 7: Craters of with different combinations of tool materials. (a) Die steel (L)-graphite (R) tool. (b) Graphite (L)-copper (R) tool. (c) Die steel (L)-copper (R) tool.

Table 5: Tool wear of the composite tool combined with different materials.

Composite tool	Graphite-die steel		Graphite-copper		Die steel-copper	
	Graphite	Die steel	Graphite	Copper	Die steel	Copper
Volume removal (μm^3)	438	1308.5	109	526.3	503.75	576.5

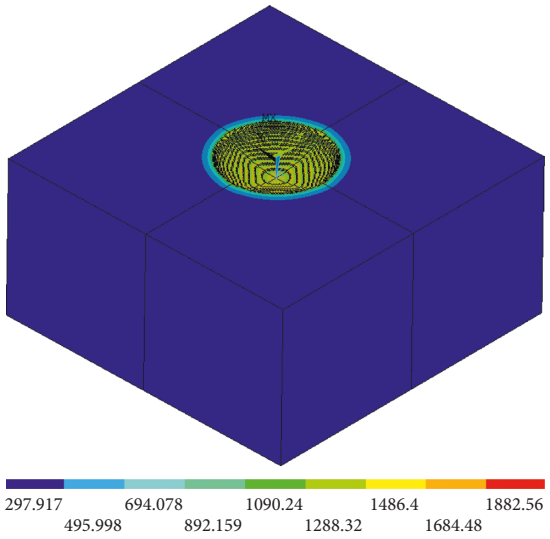

Figure 8: Temperature contour of die steel workpiece.

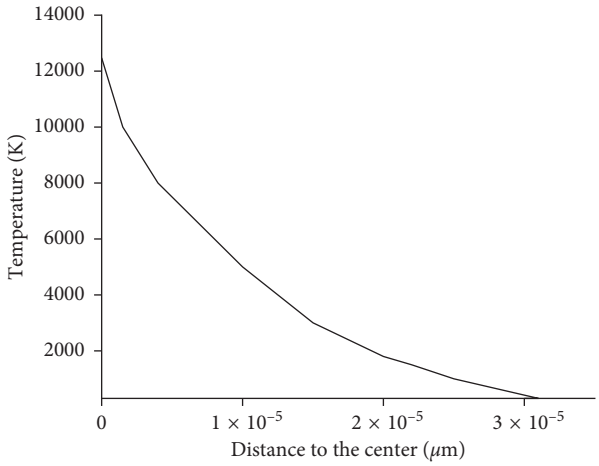

Figure 9: Temperature curve of die steel workpiece.

temperature is very high, so there is little time for the heat to conduct to other regions.

4. Multimaterial Tool Processing Experiment

4.1. Experimental Setup. In this paper, the interaction between the matrix material and the reinforcement material during the microdischarge material removal process of the composite material was studied. However, this microdischarge process could not be verified by experiments directly. Therefore, we designed a multimaterial electrode discharge experiment to investigate the removal law of different materials during the microdischarge process of composite materials by observing removal result.

The two-electrode materials (copper and die steel) were connected with tin material to form multimaterial electrode by hot-dip coating. And the die steel was processed with fabricated multimaterial electrodes in EDM without flushing. Besides, the simulations studied a microthermal distribution of volume removal process; however, it was hard to calculate the removal volume within one pulse, and it was difficult to ensure that the discharge point was located just in the middle of the two materials in the experiment. So, this paper designed a multimaterial electrode for experiment with continues discharging machining. After machining, the total removal volumes of electrodes were obtained, and a single discharge-removal volume was worked out. And, compare the experimental removal volume with simulations.

The thickness of die steel workpiece was 15 mm, and the dielectric was deionized water. The machine was a self-built desktop EDM sinking machine, which consisted of automatic feeding device, power supply, and worktable as shown in Figure 10. The experimental parameters of EDM using multimaterial electrodes are shown in Table 6.

4.2. Experimental Results and Discussion. The multimaterial electrodes were weighed and the length of multimaterial electrodes was measured before and after machining. And the average values were calculated. The die steel was

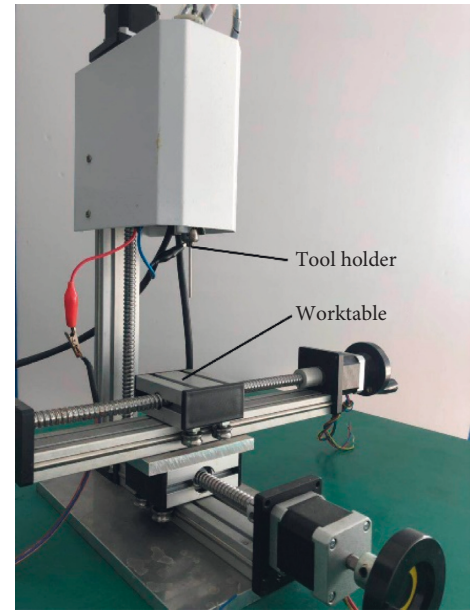

Figure 10: Self-built EDM sinking machine.

Table 6: Material parameters and electrical parameters of EDM experiments.

Parameters	Value
Materials of electrodes	Copper and die steel
Materials of workpiece	Die steel
Machining polarity	Negative
Pulse on time	20 μs
Pulse off time	10 μs
Breakdown voltage	20 V
Peak electric current	1.4 A
Diameter of electrodes	2 mm
Machining time	180 s
Dielectric	Deionized water

processed under the condition where the breakdown voltage was 20 V, the peak current was 1.4 A, the pulse width was 20 μs, and the processing time was 180 s. Figure 11 shows the multimaterial electrodes before and after machining. Figure 12 shows the appearance of the workpiece and the measurement of the workpiece after machining.

The total wear of the die steel tool and the copper tool is slightly less than the total wear of the multimaterial tool, which could be because of the influence of the bonder. Due to the small size of bonder, the influence of the bonder can be ignored. Then, equation (19) can be used to calculate the wear volume under the single-pulse discharge condition:

$$v = \frac{(t_{on} + t_{off})}{t} V, \tag{19}$$

where t_{on} is the pulse width, μs; t_{off} is the pulse interval, μs; t is the total processing time, s; V is the total volume removed, μm^3; and v is the volume removal per discharge, μm^3. Table 7 shows the average values of electrodes before

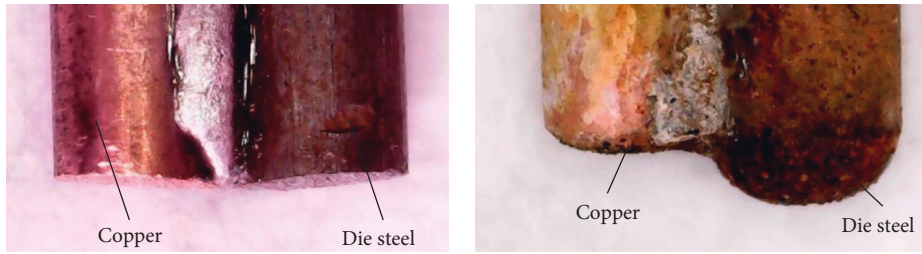

(a) (b)

Figure 11: Multimaterial electrodes before and after machining. (a) Before machining. (b) After machining.

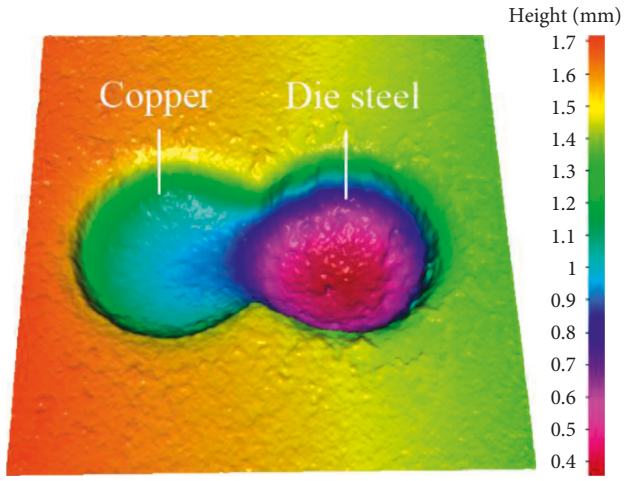

Figure 12: Die steel workpiece appearance after machining.

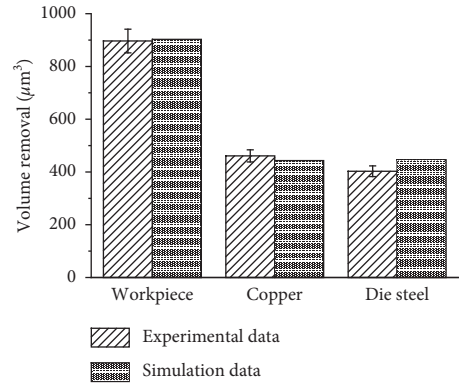

Figure 13: Multimaterial tool simulation and experimental data.

Table 7: Wear of multimaterial electrodes.

Parameters	Copper	Die steel
Average original length (mm)	44.89	46.39
Average after processing length (mm)	43.95	45.58
Average length difference (mm)	0.94	0.81
Average original weight (g)	1.2629	1.1537
Average after processing weight (g)	1.2396	1.1336
Average weight difference (g)	0.0264	0.0201

Table 8: Multimaterial tool simulation and experimental data.

Tool material	Simulation data (μm^3)	Average experimental data (μm^3)	Error (%)
Die steel	403	446.56	9.75
Copper	461.2	443.18	3.91
Die steel (Workpiece)	896.66	903.00	0.70

and after machining. Figure 13 shows the errors and average values of different material removal volumes in experiments. The average experimental volumes removed per discharge of die steel tool, copper tool, and workpiece are 446.56 μm^3, 443.18 μm^3, and 903.00 μm^3. The largest errors of copper, die steel, and workpiece are 5.87%, 9.35%, and 4.70%, respectively, which shows better accurate results. Table 8 shows the simulation data and average experimental data. The simulation volumes removed per discharge of die steel tool, copper tool, and workpiece are 403 μm^3, 461.2 μm^3, and 896.66 μm^3. Considering that not all the discharge pulses are effective during the process, this paper takes 80% as the utilization rate for the discharge pulses to simulate the removal volume of the electrodes.

By observing the simulation and experimental data in Figure 13 and Table 8, it is found that the simulation data obtained under the single-pulse condition are close to the experimental data of a multimaterial tool. As a result of the finite element method for simulation analysis, it is impossible to completely apply the boundary conditions according to the actual working conditions, only by applying boundary conditions as close as possible to the actual working conditions. Additionally, in the actual process, parameters are not constant, but in simulations, the average parameters are selected to reflect the actual working conditions, so there will be some errors. However, the simulation volume removal is very close to the experimental wear volume, the errors between simulations and experiments of die steel, copper, and die steel (workpiece) are 9.75%, 3.91%, and 0.70% separately, which are all less than 10%, indicating that the simulation model is effective, and it can be used to predict the multimaterial tool wear rate.

5. Conclusions

In this paper, the discharge channel and convective heat transfer in EDM with composite tools are simulated, and the

temperature distribution of the tool surface after the application of the heat flux density is obtained. The craters of the composite tool were obtained by the method of element birth and death, and then, the wear volume was calculated and analyzed. And the simulation results are verified by experiments. The following conclusions are obtained by analyzing and comparing the simulation results of composite tool:

(1) The highest point of the composite tool temperature of the copper-die steel is not at the center of the heat flux density, but deviates on the die steel tool with the poor thermal conductivity.

(2) The volume wear of composite tool will increase with the increase of current, voltage, and pulse width.

(3) In the case of copper-die steel composite tool, in a certain range of energy, the copper tool wear volume is smaller than the die steel, but when the discharge energy increases, the wear of the copper tool is higher than die steel.

(4) It is proved that the simulation can predict the removal volume of the composite tools. The error of simulation is less than 10%, indicating that the simulation model is effective.

Data Availability

The data used to support the findings of this study are available from the corresponding author upon request.

Conflicts of Interest

The authors declare that there are no conflicts of interest regarding the publication of this paper.

Acknowledgments

The financial support from the National Natural Science Foundation of China under grant no. 51875074, Scientific Research Platform Foundation of Liaoning Province under grant no. JDL2016006, and General Program of Natural Science Foundation of Liaoning Province under grant no. 20180550425 is acknowledged.

References

[1] S. Norasetthekul, P. T. Eubank, W. L. Bradley, B. Bozkurt, and B. Stucker, "Use of zirconium diboride-copper as an electrode in plasma applications," *Journal of Materials Science*, vol. 34, no. 6, pp. 1261–1270, 1999.

[2] H. C. Tsai, B. H. Yan, and F. Y. Huang, "EDM performance of Cr/Cu-based composite electrodes," *International Journal of Machine Tools and Manufacture*, vol. 43, no. 3, pp. 245–252, 2003.

[3] A. K. Khanra, B. R. Sarkar, B. Bhattacharya, L. C. Pathak, and M. M. Godkhindi, "Performance of ZrB2-Cu composite as an EDM electrode," *Journal of Materials Processing Technology*, vol. 183, no. 1, pp. 122–126, 2007.

[4] T. A. El-Taweel, "Multi-response optimization of EDM with Al-Cu-Si-TiC P/M composite electrode," *The International Journal of Advanced Manufacturing Technology*, vol. 44, no. 1-2, pp. 100–113, 2008.

[5] N. H. Hassan, M. N. Zain, M. S. Wahab et al., "Fabrication of MMC material for EDM electrode," in *Proceedings of 2009 IEEE Student Conference on Research and Development (SCOReD)*, pp. 262–265, Selangor, Malaysia, November 2010.

[6] V. Senthilkumar and M. C. Reddy, "Performance analysis of Cu-B," *International Journal of Machining and Machinability of Materials*, vol. 11, no. 1, pp. 36–50, 2012.

[7] P. Goyal, "Enhancement of MRR in EDM by composite material electrode on die steel," *International Journal of Science, Engineering and Technology Research*, vol. 3, no. 10, pp. 2640–2643, 2014.

[8] A. H. Chiou, C. C. Tsao, and C. Y. Hsu, "A study of the machining characteristics of micro EDM milling and its improvement by electrode coating," *International Journal of Advanced Manufacturing Technology*, vol. 78, no. 9–12, pp. 1857–1864, 2015.

[9] M. Z. Hussain, U. Khan, R. Jangid et al., "Hardness and wear analysis of Cu/Al_2O_3 composite for application in EDM electrode," *IOP Conference Series: Materials Science and Engineering*, vol. 310, no. 1, article 012044, 2018.

[10] S. Zhang, Y. Liu, W. Zhang et al., *Multi-Material EDM Tool and Its Processing Method*, China Patent, ZL201610839663.1, 2018, in Chinese.

[11] S. Joshi and S. Pande, "Development of an intelligent process model for EDM," *International Journal of Advanced Manufacturing Technology*, vol. 45, no. 3-4, p. 300, 2009.

[12] J. F. Liu and Y. B. Guo, "Thermal modeling of EDM with progression of massive random electrical discharges," *Procedia Manufacturing*, vol. 5, pp. 495–507, 2016.

[13] X. Wang, H. Hu, Y. Liang et al., "Finite element simulation of small-hole on titanium alloy drilled by EDM," *China Mechanical Engineering*, vol. 24, no. 13, pp. 1738–1742, 2013, in Chinese.

[14] J. P. Holman, *Heat Transfer*, McGraw-Hill, New York, NY, USA, 2010.

[15] H. S. Carslaw and J. O. Jaeger, *Conduction of Heat in Solids*, Oxford University Press, London, UK, 1959.

[16] Y. S. Touloukian, *Conductivity Metallic Elements and Alloys*, Plenum Publishing Corporation, New York, WA, USA, 1970.

[17] M. Bhaumik and K. Maity, "Effect of different tool materials during EDM performance of titanium grade 6 alloy," *Engineering Science and Technology, an International Journal*, vol. 21, no. 3, pp. 507–516, 2018.